



HAL
open science

Influence of vegetation-induced water table seasonality on groundwater chloride concentration dynamics in a riparian fen peatland

Adrien Renaud, Véronique Durand, Claude Mügler, Christelle Marlin,
Emmanuel Léger, Aurélie Noret, Gaël Monvoisin

► To cite this version:

Adrien Renaud, Véronique Durand, Claude Mügler, Christelle Marlin, Emmanuel Léger, et al.. Influence of vegetation-induced water table seasonality on groundwater chloride concentration dynamics in a riparian fen peatland. *Hydrological Processes*, 2023, 37 (12), 10.1002/hyp.15054 . hal-04379483

HAL Id: hal-04379483

<https://hal.science/hal-04379483>

Submitted on 8 Jan 2024





HAL is a multi-disciplinary open access archive for the deposit and dissemination of scientific research documents, whether they are published or not. The documents may come from teaching and research institutions in France or abroad, or from public or private research centers.

L'archive ouverte pluridisciplinaire **HAL**, est destinée au dépôt et à la diffusion de documents scientifiques de niveau recherche, publiés ou non, émanant des établissements d'enseignement et de recherche français ou étrangers, des laboratoires publics ou privés.

RESEARCH ARTICLE

WILEY

Influence of vegetation-induced water table seasonality on groundwater chloride concentration dynamics in a riparian fen peatland

Adrien Renaud^{1,2}  | Véronique Durand¹  | Claude Mügler²  |
Christelle Marlin¹ | Emmanuel Léger¹  | Aurélie Noret¹ | Gaël Monvoisin¹

¹Laboratoire GEOPS, Université Paris-Saclay, CNRS, Orsay, France

²Laboratoire des sciences du climat et de l'environnement, Université Paris-Saclay, CNRS, CEA, UVSQ, Gif-sur-Yvette, France

Correspondence

Adrien Renaud, Laboratoire GEOPS, Université Paris-Saclay, CNRS, Orsay, 91405, France.

Email: adrien.renaud@proton.me

Funding information

Université Paris-Saclay

Abstract

Peatlands are environments that rely mainly on high water levels to accumulate organic matter. Depending on the chemical species observed, the lowering of the water table can change biogeochemical equilibria, with various impacts. This paper aims to understand the effect of shallow groundwater seasonality on chloride concentrations in a French riparian peatland by combining water table monitoring, geochemical and stable water isotopes analysis. Water table levels and groundwater samples were recorded and collected for 3 years, every 2 months, in nine observation wells and the nearby river. Chloride concentrations were highly variable in space and time, ranging from 10 to 100 mg L⁻¹. They are shown to be related to the water table dynamics, which are closely linked to the life cycle of the local vegetation. These dynamics were characterized by a significant drawdown between June and October due to plant transpiration and a fast recovering period just after its senescence. Results show that the chloride accumulates within the unsaturated zone during the drying phase and is solubilized back into the groundwater during the rewetting phase, increasing its concentration. Moreover, the water table rises in autumn with various dynamics according to the location in the peatland, which induces some special differences in hydraulic gradients. Such gradients allow lateral transfers from zones of fast recovery to zones of slow recovery, where year-to-year chloride accumulation was observed. These complex 3D processes preclude the use of chloride to constrain how the peatland hydrogeological system functions. Conversely, the use of stable water isotopes in this work emphasizes the importance of the river's role during the summer as a water supplier to counterbalance vegetation transpiration.

KEYWORDS

chloride, heterogeneity, isotopes, monitoring, peatland, seasonality, transpiration, water table

This is an open access article under the terms of the [Creative Commons Attribution](https://creativecommons.org/licenses/by/4.0/) License, which permits use, distribution and reproduction in any medium, provided the original work is properly cited.

© 2023 The Authors. *Hydrological Processes* published by John Wiley & Sons Ltd.

1 | INTRODUCTION

Peatlands cover only 5% of the European territory (500 000 km²) and yet they are keystone environments in the human ecosystem, acting as carbon sinks, natural freshwater reservoirs, buffer units during flood events, and biodiversity shelters for numerous endangered species (Convention on Wetlands, 2021). Peatlands are specific wetlands where carbon accumulates because of a primary production greater than the degradation losses. An essential factor controlling decomposition losses from peatlands is the depth of the seasonal minimum water table Belyea and Malmer (2004). Below this depth is the permanently saturated water table, where microbial activity and decomposition are slow due to the lack of oxygen. Changes in atmospheric conditions, for example the temperature and evapotranspiration increase predicted with global warming (IPCC, 2022), or land use modifications, such as human-induced drainage, can increase the amplitude of the seasonal fluctuations of the water table between dry and wet periods. These changes introduce oxygen into a deeper unsaturated zone in the peatland and activate the mineralization of organic matter (Charman et al., 2008; Freeman et al., 1993; Holden et al., 2003). Therefore, these changes in water table depths impact the main biogeochemical cycles (e.g., sulfur Urban et al. (1989), Warren et al. (2001), De Ridder (2012), nitrogen (Rubol et al., 2012) and carbon cycles (Blodau et al., 2007)), but they also affect other geochemical species such as chloride.

Chloride in groundwater is often hydrologically considered a conservative element, meaning it does not interact with the soil matrix or other compounds during water transport. Consequently, it can be used as a natural tracer to determine the origin of water and how the distinct sources are mixed together (Kirchner & Tetzlaff, 2010; Reddy et al., 2008). One of the processes in which chloride is not conserved is evapotranspiration, involving chloride enrichment in soil solution or groundwater compared with rainwater. Chloride moves upward in the vadose zone with capillary soil water and accumulates near the surface as water is consumed by evapotranspiration (Hayashi et al., 1998). Therefore, chloride can be used to estimate evapotranspiration rate or rainfall accumulation using mass balance calculation (Auterives et al., 2011). Vegetation can amplify this process through root exclusion, leading to high salinization rates (Grimaldi et al., 2009) depending on the plant species (Humphries et al., 2011). However, rapidly growing plants can consume large amounts of chloride as micro-nutrients (Svensson et al. (2021) and references therein). For example, Hayashi et al. (1998) observed a seasonal cycle of chloride mass in a pond. As the authors could not explain the significant decrease in chloride mass in spring by physical processes alone, they concluded that substantial uptake of chloride by plants occurred during the growing season. The chloride was then released into the pond water in autumn when most plants were senescing after the first frost. Kashparov et al. (2007) also showed that rapidly growing plants take up large amounts of chloride. The importance of chloride biological accumulation and release was also proved by experimental chloride additions to the forest floor that induced increased chloride concentration in foliage, throughfall, and soil solution (Lovett et al., 2005).

Furthermore, chloride can be involved in several retention or release processes. McCarter et al. (2019) showed that chloride adsorption is negligible at concentrations below 305 mg L⁻¹. However, natural processes of organic chloride formation (chlorination) were observed in all types of soils and ecosystems (Redon et al., 2013; Svensson et al., 2021). Chlorination, which is related to organic matter recycling (Öberg & Grøn, 1998) and to soil microbial activity (Verhagen et al., 1998), was found to be greater in litter than in deeper soil layers (Svensson et al., 2021) and mostly took place in the rhizosphere (Montelius et al., 2019). Dechlorination processes, which are the reverse processes of chlorination and allow the transition of organic forms of chloride to inorganic forms, also occur naturally in soils (Svensson et al., 2021). Simultaneous chlorination and dechlorination processes have been shown in the detached dead or dying plant biomass of litter (Myneni, 2002).

Although chloride behaviour is affected by several processes that indicate topsoil transformation, the depth to water table remains a crucial factor for the chloride concentrations in shallow groundwater. The depth to water table in peatlands is not homogeneous and depends on spatial location (Joris & Feyen, 2003), soil physical parameters (Ahmad et al., 2021), vegetation cover (Volik et al., 2020), and of course seasonal atmospheric forcings. As a consequence, its effect on the concentrations of chemical elements varies both spatially and temporally. Thus, the depth to water table has been reported as an essential parameter of soil salinization because it redistributes vertical chloride profiles (Zhao et al., 2019). Grimaldi et al. (2009) observed both a heterogeneous spatial distribution and a strong seasonality of chloride concentrations in the upper part of a shallow aquifer. The strong spatiotemporal heterogeneity was due to chloride accumulation in the unsaturated zone close to an oak hedge during the vegetation growing season, implying higher chloride concentrations within the saturated zone when the water table rose rapidly and reached this chloride-enriched root zone. Aubert et al. (2013) also observed the effect of chloride accumulation in the vadose zone by the summer evapotranspiration process results in increased chloride concentration in groundwater when the water table rises. Additionally, Humphries et al. (2011) showed that chloride concentration dynamics are not only vertical processes: the depth to water table can induce 3D chloride migration following hydraulic gradients due to heterogeneous hydraulic heads within the water body.

Understanding the hydrological functioning of the peatland is thus crucial to precisely constrain chloride dynamics. In this context, chloride is therefore no longer appropriate for tracing the origin of water since vegetation, seasonal meteorological parameters, and shallow groundwater dynamics affect its concentration. As an alternative, many studies have shown that stable isotopes of the water molecule (¹⁸O and ²H) are suitable tracers that can be used in most environments (Vreca & Kern, 2020), including riparian wetlands (Gourcy & Brenot, 2011; Quenet et al., 2019), and also peatland (Clay et al., 2004; Isokangas et al., 2017).

The present paper aims to understand the effect of shallow groundwater seasonality, induced by the vegetation uptake cycle, on chloride concentrations by combining water table monitoring,

geochemical and stable water isotopes analysis. The developed methodology involved continuous monitoring of river and aquifer water levels and groundwater sampling for isotopic and geochemical analysis.

2 | MATERIALS AND METHODS

2.1 | Site

The Jarcy peatland is an undisturbed riparian wetland located in France, 50 km south of Paris, on the right riverside of the Essonne river (48°25'31"N, 2°22'50" E, cf. Figure 1) which is one of the main tributaries of the Seine. It is about 100 km long, it flows North and drains a total catchment of about 1900 km², with 850 km² at the study site location. The Jarcy peatland is located between two dams, which maintain the river stage between 57.55 and 57.72 m above

sea level (a.s.l.) on average, with an average hydraulic gradient equal to 10–4.

The watershed is part of the major carbonate system aquifer of Beauce, a tertiary geological unit of the Paris basin. The Essonne valley is filled with modern alluvium, consisting mainly of peat material in riparian zones. The site is a minerotrophic peatland, with a peat thickness varying from 5 to almost 15 m at its center (close to s2, see Figure 2). Its 4.5 ha surface is covered mainly by *Phragmites Australis*, a common reed found in many peatland systems. The topography of the peatland is sub-planar/horizontal: the elevation ranges from 57.70 m a.s.l. to 57.96 m a.s.l. A topographical depression is located in the middle of the peatland, along an s2/s4 axis, with the lowest altitude at s4. Average annual precipitation and potential evapotranspiration (PET) during the monitoring period (2018–2021) were 567 and 865 mm, respectively. Precipitation was provided by Météo-France (French Meteorological Center) at the Courdimanche station, 600 m

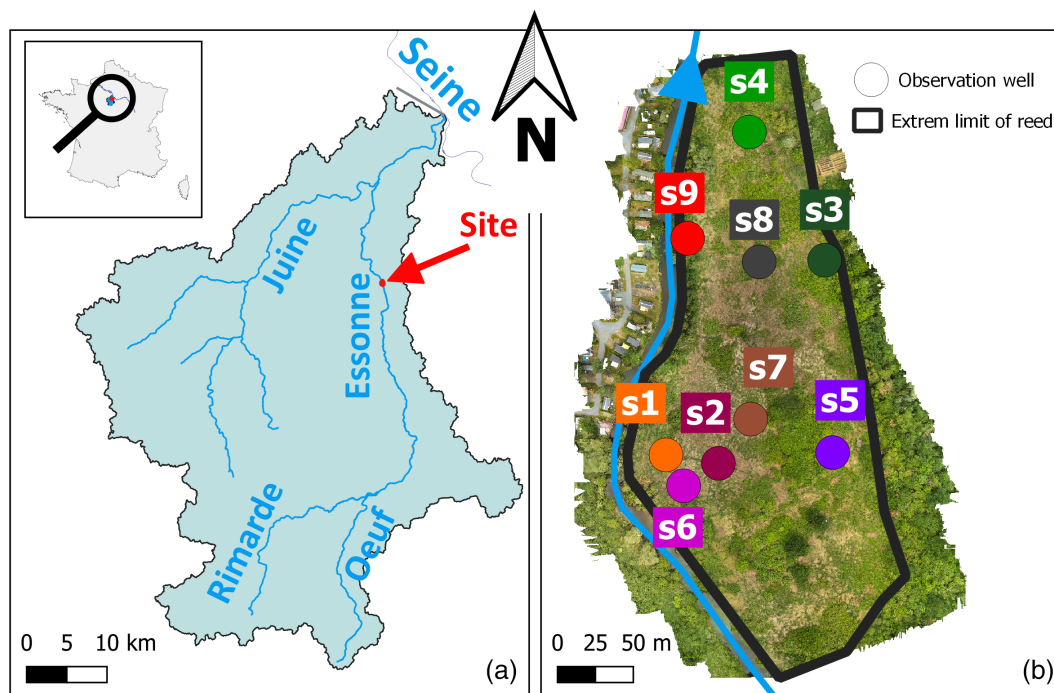


FIGURE 1 Study site: (a) large scale location and (b) aerial view of the Jarcy peatland with the piezometers' location. The Essonne river is at the peatland western boundary. The blue arrow indicates the river flow direction.

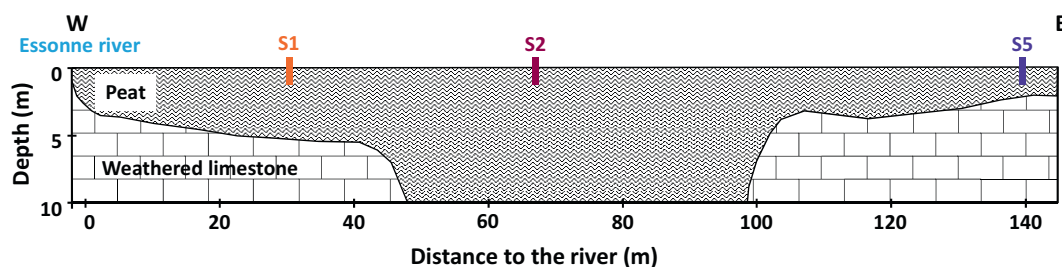


FIGURE 2 Cross-sectional view of the Jarcy fen.

from the site. PET was calculated using the Penman-Monteith method from the five closest stations in a 15 km cell grid.

2.2 | Sampling points

To investigate the groundwater level and geochemical signatures, a network of nine piezometers was installed in June 2018 in the peatland (Figure 1). Each was drilled using an auger to a 1.8 m depth and equipped with Polyethylene tubes of 5 cm in diameter, sunk directly into the holes, with screen slots from 0.2 to 1.7 m below the ground surface.

2.3 | Piezometric monitoring

Water levels were recorded continuously at a 10 min time step for seven piezometers (s1, s2, s3, s4, s5, s8, and s9 see Figure 1) using TD-Diver probes (0.05 kPa accuracy). To calculate relative water depth, the barometric pressure was recorded on-site using a Baro-Diver (vanEssen Instruments, 0.05 kPa accuracy), and all the piezometers were levelled using a Differential Global Positioning System, with an accuracy of 5 cm for the altitude. Missing values in time series of s5 and s8 are due to probe failures. Water levels were also measured every 2 months with a hand probe at each sampling point. The river stage was monitored using two pressure probes located 2 km upstream and 150 m downstream of the site, and managed by the river administrator (SIARCE). The monitoring period lasted from June 2018 to July 2021.

2.4 | Geochemical monitoring

Eighteen water sampling campaigns were performed during the 3-year monitoring period in the nine piezometers and the nearby Essonne river. Concerning the groundwater, sampling was performed using a peristaltic pump after renewing the volume of the water column three times. Water was 0.45 μm -filtered with cellulose acetate syringe filters and sampled in 10 mL HPDE tubes for anion and cation analysis and in 10 mL amber glass bottles for stable water isotope analysis. Samples for cation analysis were acidified the same day of sampling, and all samples were stored in a cool box during fieldwork and in the fridge until analysis was carried out. Ion analysis was performed on two Dionex™ ICS-1000 Ion Chromatography Systems in the GEOPS laboratory. Samples were diluted from a factor of 3 to 10 to avoid over-saturation of the chromatography column. Accuracy was about 1% for chloride. Stable water isotopes were analysed in the GEOPS laboratory by cavity-enhanced absorption spectroscopy on a TLWIA-45-EP (Triple Liquid Water Isotope Analyser) with a precision less than 0.60 ‰ for $\delta^2\text{H}$ and 0.20 ‰ for $\delta^{18}\text{O}$. To improve the readability, isotopic results for the remainder of the paper are presented as $\delta^2\text{H}/\delta^{18}\text{O}$ (‰ VSMOW) when not specified.

2.5 | Cross-correlation analysis

A cross-correlation analysis was performed between the water table elevation time series at each observation well and the PET time series. The purpose of the cross-correlation analysis was to determine the phase difference for the two signals that have the highest correlation score, meaning that the two variables are indeed correlated but with a time delay. The correlation coefficient r_i between the two series $X(t)$ and $Y(t)$ was calculated as follows:

$$r_i = \frac{\text{COV}(X'(t), Y'(t))}{\sqrt{\text{VAR}(X'(t)) \times \text{VAR}(Y'(t))}}, \quad (1)$$

where

$$\begin{cases} X'(t) = X(t) \quad \forall t \in [t_0, t_n - |i|] \\ Y'(t) = Y(t) \quad \forall t \in [t_0 + |i|, t_n] \end{cases} \quad \text{if } i < 0,$$

$$\begin{cases} X'(t) = X(t) \quad \forall t \in [t_0 + |i|, t_n] \\ Y'(t) = Y(t) \quad \forall t \in [t_0, t_n - |i|] \end{cases} \quad \text{if } i \geq 0.$$

Note that i is the lag between the two time series and $\text{COV}(x, y)$ is the covariance between the two variables x and y . $X(t)$ and $Y(t)$ must have the same length and same time step (in this paper, daily), and i (the lag) must be a multiple of the time step and can be positive or negative.

3 | RESULTS

3.1 | Water table fluctuations

The water table depths within the seven piezometers s1, s2, s3, s4, s5, s8 and s9, relative to their ground surface elevation, were found to follow a pronounced seasonality between high and low levels in winter and summer, respectively (Figure 3).

The low-level periods lasted from late June to November, and the maximum depth to water table varied from 0.8 m in s1 to 1.5 m in s2. During the high-level season, from December to March, water levels were close to the surface (depth <math><0.1\text{ m}</math>) except in s1 and s9, where the average depth was about 0.3 m. From March to June, there was a transitional period where the water table started to decline but was still able to rise quite quickly due to the numerous rainfall events.

Thanks to manual measurements during the different sampling campaigns, it was possible to have an insight of the water levels amplitudes and dynamics in s6 and s7 even if they were not equipped with pressure probes. Dynamics were identical to other piezometers with alternating between high and low water levels each year. Amplitudes in s6 looked like the s1 signal with average depth during the winter of 0.3 m, but during the summer, the maximum drawdown was actually slightly deeper (0.9 m at maximum in 2018 and 2020). s8 was more similar to the s2 signal in dynamics, notably in late November

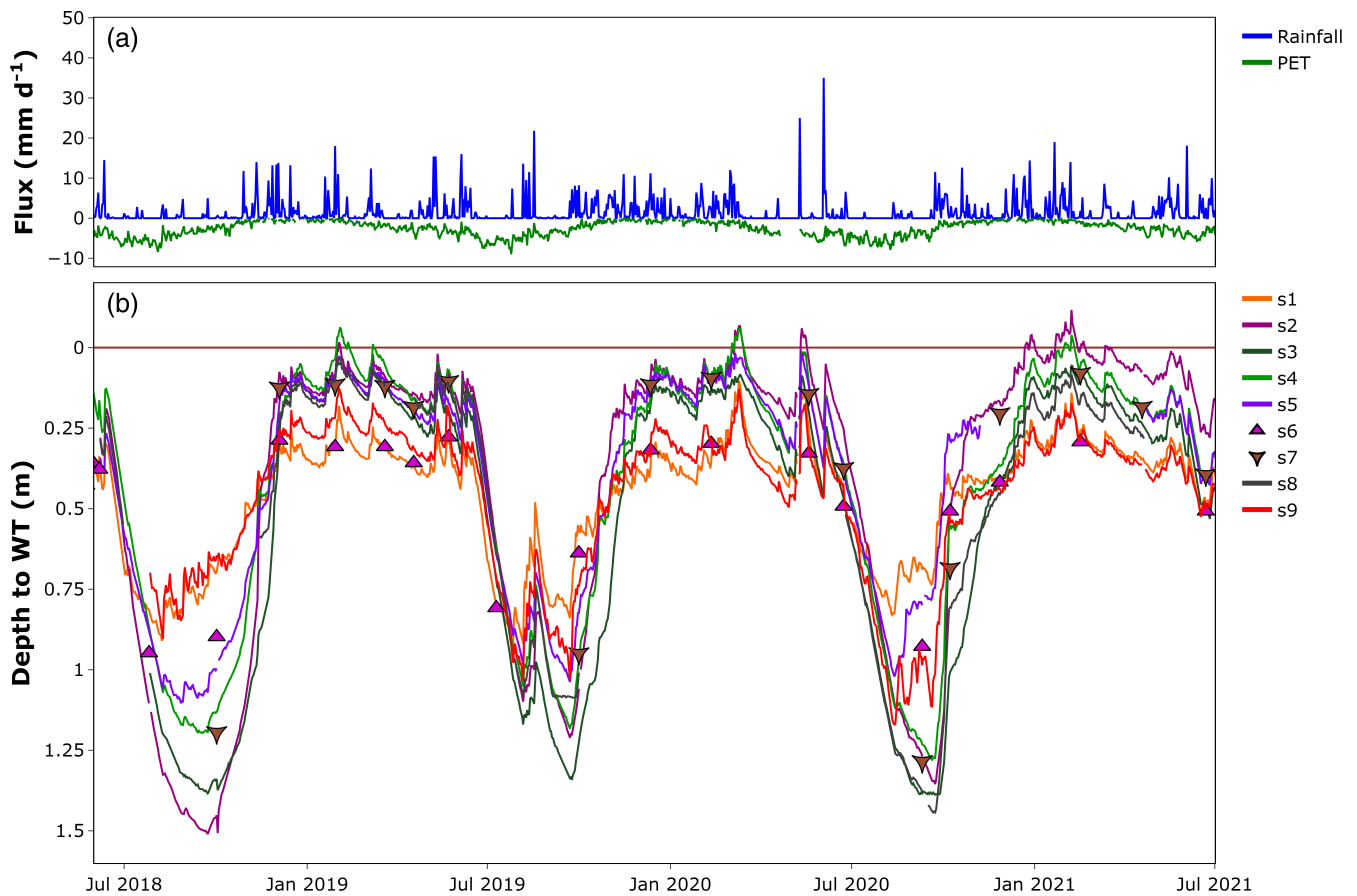


FIGURE 3 Time evolutions from June 2018 to July 2021 of the (a) daily rainfall and potential evapotranspiration (PET); (b) depth to water table (WT) in the seven piezometers equipped with pressure probes (s1, s2, s3, s4, s5, s8 and s9). Stars correspond to manual measurements in s6 and s7 wells (not equipped with probes). The horizontal brown line indicates the ground surface.

2020 where the two were the closest to the ground surface, but looked more alike s4 in amplitudes, with maximum drawdown in the same order of magnitude (1.25 m depth at maximum and 0.15 m at minimum).

The maximum drawdown was observed in the center of the peatland towards the northeast zone, including s2, s7, s8, s3 and s4. The recession dynamic was fairly similar from one piezometer to another, starting at the same time (early June of each year) with an almost identical slope (-0.02 m d^{-1} in 2018 and 2019 on average, and -0.01 m d^{-1} in 2021) until each reached its maximum drawdown. At the opposite, the rising dynamic was specific to every piezometer. Considering the start of the rise as the date when water levels stop decreasing, this moment came synchronously for all the piezometers every year (23rd, 24th and 21st of September respectively in 2018, 2019 and 2020). The duration of the rise was also similar for every monitored wells (65, 50 and 80 days respectively in 2018, 2019 and 2020), with the exception of s4 where longer recovery durations were recorded in 2018 and 2019 (75 and 65 days respectively) and s3 in 2019 (65 days). However, since maximum depth to water table varied a lot, rising rates were also very different, with a minimum value in s1 (0.006 m d^{-1} in average), followed by s9 (0.009 m d^{-1}), then s4, s3 and s5 (0.015 m d^{-1}) and s2 (0.018 m d^{-1}).

Finally, these rates were also much higher for short periods during rainy events, with values from 0.06 up to 0.17 m d^{-1} respectively in s3 and s2 for example, (25 mm of rain between 2 October and 7 October of 2020). But the water table rise was not necessarily linked to a period of increased rainfall, such as in 2018 for example where water levels rose without any rainy event (from 24th of September to 28th of October).

Looking to altitudes, the recovery pattern was nonetheless always the same from year to year with similar hydraulic gradients dynamics illustrated by the piezometric contours in Figure 4 drawn from the 2020 monitoring: the water table in the southern part of the peatland was the first to reach its pre-summer level, with a piezometric depression centered on s3. Then, this depression moved towards s4, which presented the lowest hydraulic head even during the high-level season. The hydraulic gradient between the river and the peatland varied from 1×10^{-4} in December 2019, close to the head equilibrium, with a flow direction mainly oriented from south to north, parallel to the river, to a maximum of 1.9×10^{-2} in September 2020, at the maximum water table drawdown, with flux from the Essonne river to the peatland.

Finally, a cross-correlation analysis was performed between the water table and PET time series at each observation well with

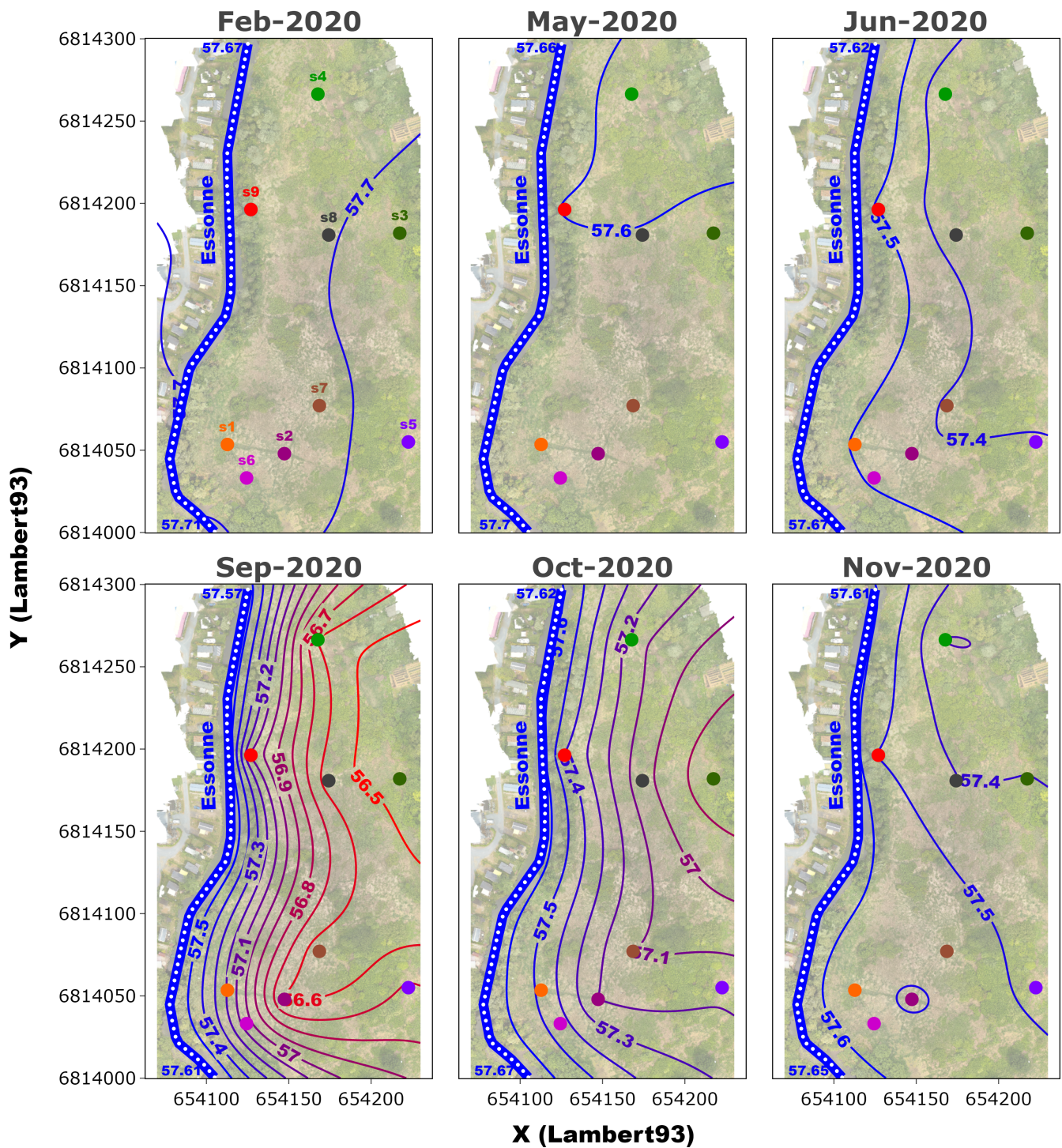


FIGURE 4 Spatial distributions of the water table levels (m a.s.l.) from (a) February 2020 to (f) November 2020. Interpolation was achieved using the Python library Scipy and its radial basis linear function interpolator. All the data available at each date were used (coloured and greyed dots for the water table within the fen, white dots for the river level).

pressure probe measurements (Figure 5). It showed that the summer drawdown is linked to the PET flux increase, the two being negatively correlated. The maximum values of the correlation coefficients are equal to -0.71 , -0.70 , -0.78 , -0.78 , -0.74 , -0.83 and -0.76 with a lag of 38, 48, 51, 50, 42, 46 and 39 days at s1, s2, s3, s4, s5, s8 and s9 respectively. The negative values of the lag reflect the delay in the response of the water table to the PET increase.

3.2 | Stable water isotopes

Figure 6a presents all the three-year monitoring isotopic data. Figure 6b-g show the same data but filtered at the six dates used to plot the piezometric contours (Figure 4, from February to November 2020). The Global Meteoric Water Line (GMWL) is plotted using Craig's equation (Craig, 1961), and Local Meteoric Water Line (LMWL;

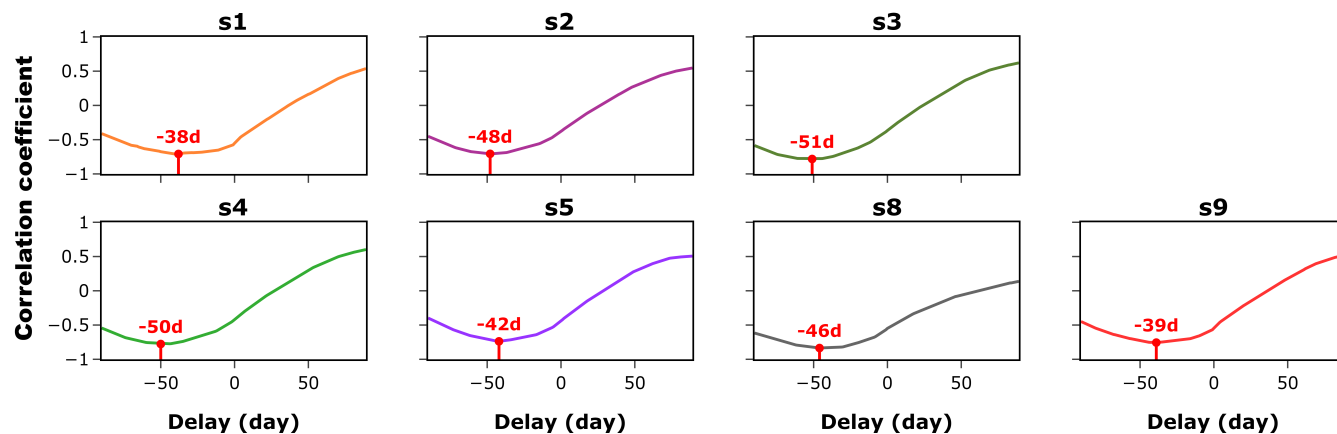


FIGURE 5 Cross-correlation between the water table and PET time series.

$\delta^2H = 7.6 \times \delta^{18}O + 6.2$, $R^2 = 0.97$, $p < 0.05$) was derived from open access data from the Fontainebleau station (RENOIR network).¹ This station is located 20 km east from the site and was operational from April 2016 to September 2018 with monthly analysis. The local mean annual rainwater signature ($-45.7/-6.9$) was also calculated from this station data using the rain volume weighted average over the available period (2016–2018). Winter recharge was calculated using the volume weighted with the same data for different periods reported in Table 1. The selected starting months (October and November) correspond to the beginning of the water table recovery (respectively early to late October). The selected final months correspond to the potential end of the period when the water table is more influenced by rainwater (December to May). Corresponding calculated winter recharge points are plotted in Figure 6b (February) and Figure 6c (May) since they are the only months that correspond to high water levels. Even if the sampling period does not fit exactly, it does give a good estimate of the different recharge signatures since they are average values spread over 2 years.

The δ^2H and $\delta^{18}O$ isotopic signatures of the Essonne river during the 2020 period (Figure 6b to g) varied between -45.5% and -41.3% VSMOW for the δ^2H and between -6.7% and -6.1% VSMOW for the $\delta^{18}O$, with mean values of $-44.1/-6.44$. Fluctuations are primarily due to a seasonal effect, with more enriched signature in summer than in winter due to both evaporation and more enriched rainwater in summer (Kirchner & Tetzlaff, 2010).

The signature of the peatland's groundwater varied much more than the river's signature and depended on the spatial location and the season. In September 2020, there were no values for both s2 and s3 because both piezometers were dried out due to a deep water level at this sampling date.

There was strong spatial heterogeneity in the peatland's signature, but all points were globally more depleted than the river (median values respectively of $-44.9/-6.7$, $-44.6/-6.6$, $-44.7/-6.6$, $-46.7/-6.9$, $-44.8/-6.5$, $-44.6/-6.6$, $-45.5/-6.8$, $-44.8/-6.6$ for s1, s2, s3, s5, s6, s7, s8 and s9), excluding s4 which was the only point where the mean water isotopic signal was higher than the river signal ($-44/-6.3$).

Regarding temporal variation, waters analysed within the peatland ranged from depleted values (minimum of $-48.8/-7.4$ in s1 in February 2020) to more enriched values (maximum of $-43.1/-6.1$ in s4 in June 2020). Other values were between those two, more or less enriched depending on the observation point, following a similar pattern from one year to another (cf. Appendix A with the entire 3-year monitoring dataset). From June to November, the groundwater signature was getting closer to the river signature, or more enriched for s4, but from February to May, they all became more depleted than the river, with even more negative values for s1 and s2 than s3 and s4, these last two remaining close to the river signature. s5 is a bit particular with the same seasonal pattern as the others but always more depleted, as the median value underlined it (with an exception in February 2020).

Samples in $\delta^{18}O$ vs. δ^2H graphs do not align to either the GMWL or LMWL. However, they tend to be aligned each month (thick red line in Figure 6, $\delta^2H = 5.13 \times \delta^{18}O - 10.99$, $p < 0.05$, $N = 99$: i.e., all the peatland and river samples of the three-year monitoring) between a rainwater winter recharge point, within the dark blue ellipse in Figure 6, depending on the period of recharge considered (Table 1), and the Essonne river signature.

3.3 | Chloride concentration fluctuations

Chloride concentration in the Essonne river varied very little (Figure 7). Its average value was equal to 0.83 meq L^{-1} (standard deviation: 0.10 meq L^{-1}). The spatial distribution of the chloride concentrations within the shallow groundwater was heterogeneous (Figure 7): as with the isotopic signature, variability depended on the monitoring location and the sampling season.

Concentrations in s1, s5, s6 varied the least (mean values of respectively $0.58 \text{ } 0.05$, $0.7 \text{ } 0.1$ and $0.6 \text{ } 0.09 \text{ meq L}^{-1}$) compared to s3, s4 and s8 where variations were the highest (respectively $1.62 \text{ } 0.58$, $1.23 \text{ } 0.41$ and $0.75 \text{ } 0.28 \text{ meq L}^{-1}$), with maximum chloride concentration values up to 1.5 , 2.1 and 2.8 meq L^{-1} (in s8, s4 and s3, respectively). In s2 and s7, variations were less pronounced ($0.60 \text{ } 0.15$ and $0.66 \text{ } 0.15 \text{ meq L}^{-1}$).

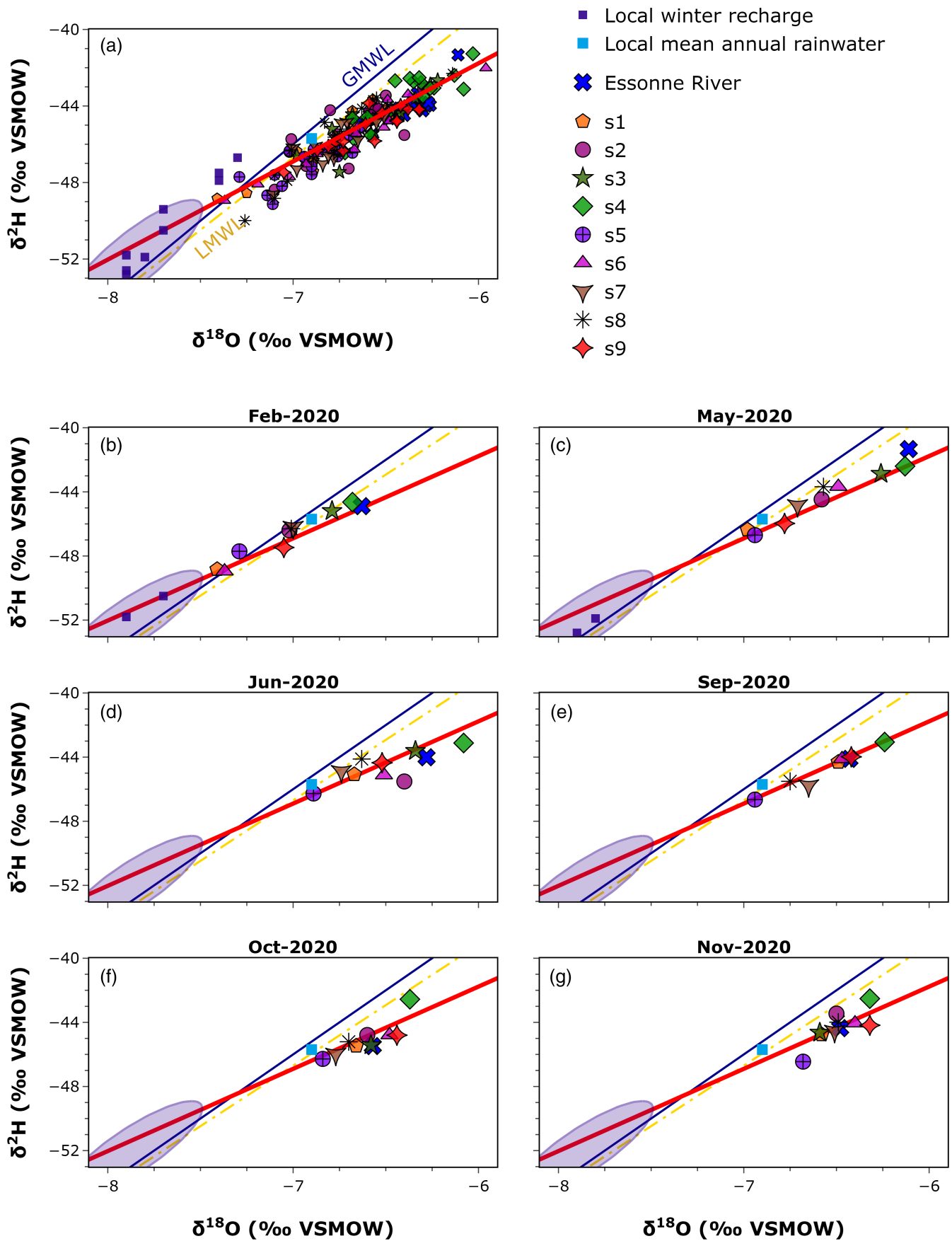


FIGURE 6 Legend on next page.

TABLE 1 $\delta^{18}\text{O}$ and $\delta^2\text{H}$ (‰ VSMOW) signature for various winter recharge periods.

Period of recharge	$\delta^{18}\text{O}$	$\delta^2\text{H}$
Oct. to Dec.	-7.4	-47.5
Oct. to Jan.	-7.3	-46.7
Oct. to Feb.	-7.7	-50.5
Oct. to Mar.	-7.9	-52.6
Oct. to May	-7.1	-46.5
Nov. to Dec.	-7.7	-49.4
Nov. to Jan.	-7.4	-47.9
Nov. to Feb.	-7.9	-51.8
Nov. to Mar.	-8.0	-53.6
Nov. to May	-7.6	-49.7

The almost same seasonality pattern was observed for s2, s3, s4, s7 and s8: concentrations decreased in summer, along with the water table drying stage, with minimum values in October. Then concentrations increased with the rise of the water table, with maximum values when water levels rose close to the ground surface. There were nevertheless some minor disparities: maximum value in s2 and s7 was reached as soon as the water table was close to the ground surface (<10 cm) and then declined gradually from January to October. In s4 and s8 on the other hand, similarly to the decreasing phase, the increase was also gradual after the rewetting phase (November) and until spring. To finish with these local disparities, concentrations in s3 increased as soon as the water table reached 0.5 m depth (see November 2020), and concentrations continued to rise until the end of the high-level phase when they dropped suddenly.

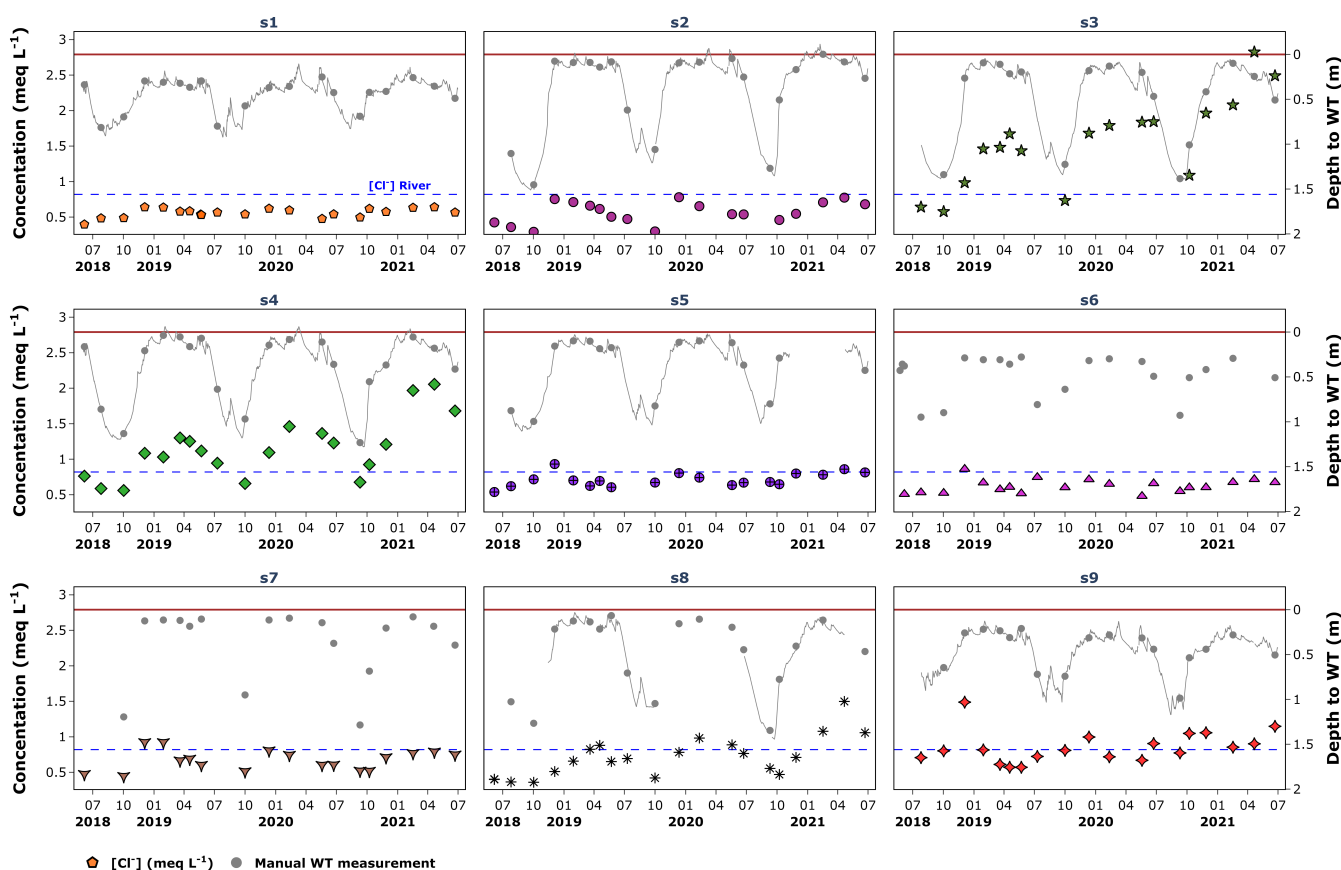


FIGURE 7 Chloride concentrations measured during the 18 campaigns of water sampling at the nine different places in the peatland (coloured points), and time evolutions from June 2018 to July 2021 of the depths to water table (continuous lines). The dashed horizontal blue line indicates the average value of the chloride concentration in the Essonne river. The horizontal brown line indicates the ground surface.

FIGURE 6 (a) $\delta^{18}\text{O}$ versus $\delta^2\text{H}$ for the three-year monitoring. The dark blue ellipse represents the local winter recharge and small dark blue squares its calculated values (see Table 1). The light blue square represents the local mean annual rainwater signature. The thick red line was obtained by linear regression with only the river and peatland data ($N = 99$, $R^2 = 0.83$, $p < 0.05$). (b) to (g) are $\delta^{18}\text{O}$ versus $\delta^2\text{H}$ for the 2020 monitoring year. Dates correspond to the water table contours in Figure 4. Regression line and local mean annual rainwater have been added each time. Local winter recharge points are displayed only for February and May campaigns.

Furthermore, chloride concentrations in s3, s4 and s8 significantly increased during the last 3 years, which was confirmed with a linear regression model (R^2 of 0.46, 0.60 and 0.38 respectively). No other sampling points showed similar behaviour.

Comparing with the river signature, observation wells in the peatland are far from having the same chloride signature. Some observation wells have lower chloride concentrations than the river (s1, s2, s5, s6 and s7), and for those with high chloride seasonality (s2, s7 and s8), this is particularly true at the end of the dewatering phase. Conversely, some observation wells (s3, s4, s8 and s9) show higher concentrations than the river, at least after the water table has risen (s8, s9), and until the next summer (s3, s4).

Each observation well seems to have its own chloride dynamic, but three different groups stand out considering only the chloride dynamics and amplitudes: s1, s5, s6 (absence of seasonality); s2, s7 (low amplitudes, clear seasonality); s3, s4, s8 (medium to high amplitudes, clear seasonality). Only s9 is out of this grouping since seasonality is not clear and concentrations are close to the river signature, sometimes above, sometimes below.

4 | DISCUSSION

Both water table and chloride concentrations are subject to strong seasonality but with significant spatial disparities. The following discussion will show at first how the vegetation controls the dynamic of the water table, and then how these dynamics impact chloride concentrations through two main processes: salinization and hydrological transfers.

4.1 | Transpiration as the water table driving force

Seasonal water table fluctuations in the Jarcy peatland were significant, between 0.6 m near the river (s1 in Figure 3) and 1.5 m in the middle of the peatland (s2 in Figure 3). These fluctuations are in the upper range of what can be found in the literature for similar environments:

- less than 0.5 m (Griffiths et al., 2019; McLaughlin & Webster, 2010),
- between 0.5 and 1 m (Auterives et al., 2011; Burt et al., 2002; Carlson Mazur et al., 2014; Cirkel et al., 2014; Ng et al., 2017),
- greater than 1 m (Clement et al., 2002; Schilling, 2007).

This high water table dynamic is mainly due to the effect of the vegetation transpiration during its growth period.

4.1.1 | Isotopes monitoring

Looking at the stable water isotopes signals, results do not show a clear evaporative signal, inducing that transpiration should be the major component of evapotranspiration since it does not imply isotopic fractionation (Liebhard et al., 2022; Zimmermann et al., 1968).

Indeed, the red regression line in Figure 6), which was derived from the whole data set and represents the average behaviour within the peatland, is more likely to be a mixing trend between two poles, the winter recharge and the river, than an evaporative line. The mixing dynamic observed in the 2020 monitoring (Figure 6b-g) between these two poles shows a yearly pattern, which can be explained as follows.

From July to January, the observation points are close to the Essonne river signal, imprinting its isotopic signature to the peatland groundwater during the whole drawdown until the rewetting period. The fact that s5 has always a more depleted signal than the river can be explained because it is hydrologically disconnected from it due to the piezometric depression centered on the peatland, as contour maps of the 2020 clearly show it (cf. Figure 4). After getting closer to the river, the peatland isotopic signature moves towards the depleted winter recharge pole (indicated by the dark blue squares in Figure 6b). This rainfall imprint was not directly observed after the rewetting period, but later in February of each year (Appendix A), implying that it takes some time for both groundwater and rainwater to mix. Similarly, after the water table starts to decrease (between May and June), the river imprint is not immediate.

Mixing is thus not a dichotomous process between only the two poles of rainwater and river water: this is due to the fact that there is always a depletion (or evaporation) gradient between the peatland sampling points while the same meteorological forcing constrains them. The fact that s4 always exhibits the most enriched signal can manifest as the peat soil structure being more subjected to evaporation (Balliston & Price, 2020). Also, because they follow two consecutive periods of short droughts (March/April and May 2020) and heavy rainfall (10 May 2020 and 3 June 2020 in Figure 3) with a shallow water table (above 0.5 m depth), the unique evaporated signatures observed in s2 and s3 in June 2020 suggest that water table dynamics under high atmospheric flux contrasts can lead to a greater isotopic variability. Even if there is no clear consensus on the processes, it has already been shown that immobile water versus mobile water within the unsaturated zone is significant in the isotopic signature of the groundwater (Renee Brooks et al., 2010; Vargas et al., 2017). When the water table rises, river water and rainwater are also mixed with the water stored within the unsaturated zone, whose isotopic signature can reflect evaporative processes or recharge inputs. This effect can explain the year-to-year variability of both transitioning phases, just after the rewetting period (end of November to January) and when the water table decreases but is still close to the ground surface (May to June). However, even if evaporation is observed, it is limited here since sampling points are rarely below the mixing line (Figure 6).

4.1.2 | Cross-correlation analysis

The cross-correlation analysis strengthens the assumption that vegetation is the main driver of the water table dynamics. The counter-correlated relation between piezometric and PET time series only found for a significant lag (from one to almost 2 months) indicates that

atmospheric loss is not directly linked to PET through evaporation since the latter is related to a fast energetic rebalance between land and atmosphere (Heitman et al., 2008). Here the delay is much more linked to the growth dynamics of reeds, which starts approximately between late May and early June, as observed during the three-year monitoring and also described in the literature (Engloner, 2009), even if it also depends on both air temperatures and water table depth (Gaberšček et al., 2020).

4.2 | Specific behaviour of chloride in-site

Chloride concentration in the Essonne watershed are relatively high (0.83 meq L⁻¹ in the Essonne River) compared to rainwater, which is < 0.07 meq L⁻¹ in the region (according to Beysens et al. (2017), measured from April 2011 to March 2012 on a site located 45 km north from the Jarcy peatland). The intensive agricultural practices could partly explain this difference between the concentrations in rainwater and in the stream in the Essonne watershed since chloride is a component of some fertilizers (KCl based, e.g.).

Isotope analysis has shown that the river and precipitation are the main source of water for the fen in summer and winter respectively. However, chloride concentrations are not the result of a simple mixing between these two poles.

In fact, chloride concentrations below the river signature are not due here to a dilution effect with rain water since the lowest concentrations correspond to the period of low water levels, when the groundwater in the peatland is mainly fed by the river: concentrations should instead be closer to the river signature, or at least increase towards it. This indicates that there is a process retaining chloride within the porous matrix. Few authors observed such retention due to organic-bounded chloride through chlorination process (Biester et al., 2006; Gustavsson et al., 2012; Redon et al., 2013), which could explain these low concentrations.

Conversely, chloride concentrations above the river signature (and thus rain water signature) indicate that there must exist another mixing pole with a high chloride concentration. This seems to be more likely the case for s2 and s7 also, even if concentrations do not exceed the river signature, since as explained before, they are not linked to the end of summer inputs of river water. Moreover, the year to year maximum concentrations increase in s3, s4 and s8 points out that chloride accumulates within the peatland, at least over the monitoring period. As introduced at the beginning of this discussion, these behaviour are mainly linked to the water table dynamics through two kinds of processes: the first one is the salinization within the unsaturated zone, and the second one the chloride transfer due to asynchronous water table uplift.

4.3 | Chloride concentration, water levels and salinization

The main process that explains the sharp increase in chloride observed after the rewetting period is the salinization. Since high

plant, transpiration with substantial water table drawdown occurs during the summer, a large volume of water moves upward by capillarity under the effect of transpiration, as well as rainwater, which is kept within the unsaturated zone and used by vegetation. As the volume of water within the vadose zone decreases, concentrations increase and chloride accumulates through root exclusion (Grimaldi et al., 2009; Hao et al., 2015; Humphries et al., 2011). Finally, when the water table rises, this accumulated chloride is solubilized back into the groundwater, increasing its concentrations as observed in five sampling points (s2, s3, s4, s7 and s8). The low chloride concentrations measured in s1 and s6 can be associated with the low water levels in winter, 0.3 m deep on average compared to other piezometers where depth from the ground surface to the water table is close to zero (Figure 7). Since at these two locations the water table never reaches the surface, always remaining at a depth greater than 0.3 m, the chloride is accumulated mainly within the upper first decimetres of soil and is never leached by groundwater. This can also explain the low variations and the absence of clear seasonality in s9 even if concentrations are a bit higher, closer to the river mean value. Moreover, this particular piezometer is very close to the river bank, which shows a slightly different vegetation (trees), with a potential distinct chloride dynamic.

A threshold effect between depth to the water table and chloride concentration is observed in s2 and s7, particularly in 2020 when the water level rose more slowly (Figure 3). The sampling was performed when the water table was deeper than usual (0.17 m and 0.21 respectively the 27th of November 2020 compared to approximately 0.1 m for both points in other years). Chloride concentration was at its lowest value for this period (respectively 0.54 and 0.7 meq L⁻¹ compared to 0.78 and 0.92 meq L⁻¹ the 12 December 2018 and 0.75 and 0.81 meq L⁻¹ the 12 April 2019), implying that chloride accumulates at this sampling point mainly within the first 15 cm of soil. However, no threshold effect was observed in s3, s4 or s8. In s3, concentration was lower in December 2018 and 2019 (respectively 1.0 and 1.7 meq L⁻¹) than in late November 2020 (2.0 meq L⁻¹), whereas measurements were done at a shallower groundwater level (<0.19 m deep in December 2018 and 2019, versus 0.4 m in November 2020). The same observation was made in s4 and s8 between 2018/2019 and 2020. One interpretation is that the vertical chloride profile is different for these three sampling points because chloride accumulation throughout evaporation/transpiration is not always circumscribed to the topsoil, as Zhao et al. (2019) have shown in their mesocosm experiment. Another interpretation, which can be related to the previous one, is linked to the root distribution, which might be different at these locations (s3, s4 and s8) and thus induced a distinct vertical chloride distribution, as Hao et al. (2015) demonstrated.

But since concentrations continue to increase during winter and spring, while at the same time water levels are already at their maximum (i.e., close to the ground surface), chloride solubilization in the unsaturated zone cannot be the only process that increases the chloride concentration in s3, s4 and s8. If salinization can explain the low and constant concentrations in s1 and part of the dynamics in s2, it does not explain the disparities between the various variations of amplitudes in s2, s3 and s4.

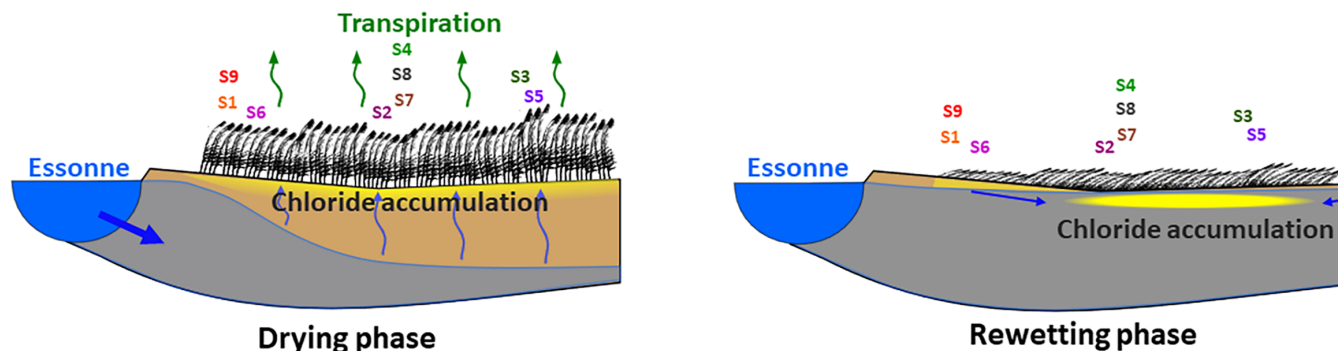


FIGURE 8 Conceptual model of the chloride behaviour between the drying and the rewetting phase.

4.4 | Water table uplift dynamics and chloride transfer

As shown previously, each piezometric signal showed a distinct rising pattern during the rewetting period (Figure 4), implying variations in hydraulic gradient between the sampling points. With the exception of 2018, hydraulic heads were always higher in s2 than in s3 and s4 during the rewetting phase, with much faster recovery rates (Figure 3). This uplift dynamic allowed groundwater to flow in a particular pattern that was almost the same each year (Figure 4). At first, s3 is in the center of the piezometric depression, with hydraulic gradient from s2, s7, s8 and s4 towards s3 ranging at maximum from 0.002 to 0.003 m m^{-1} , generally from October to late November. Then, the recovery rate in s4 decreases, becoming the new center of the piezometric depression with gradient ranging at maximum from 0.001 to 0.002 until May. Since water table recovers faster and earlier in the upstream zone of the peatland (see Figure 4), chloride that accumulates there, within the unsaturated zone, is also solubilized earlier than in the downstream zone (where s3 and s4 are located). Then, it is flushed by advection from s2 towards s3 mainly, then s4, and in the two cases via s7 and s8 following the hydraulic gradients presented before. This process can explain the progressive increase in chloride observed in s4, s7 and s8 even after the water table has risen, reaching its maximum in March instead of December, just after the rewetting period. Such chloride plume transfer due to a piezometric depression has already been reported in the literature (Humphries et al., 2011). In addition, because of this remaining piezometric depression near s4 and the near-horizontal piezometric surface, chloride is not totally flushed from the system and thus can accumulate near s3, s4 and s8, explaining the year-to-year increase observed since 2018. However, without flushing process, chloride concentration is expected to increase in the fen over time, and reaching as high values as reported by Grimaldi et al. (2009) (almost 30 meq L^{-1}). Conversely, at the beginning of the groundwater geochemical monitoring, concentrations are not so far from the regional signature (represented by the Essonne river), at least for s4, chloride concentration in s3 was already slightly higher. One hypothesis is that chloride concentrations could have been reset during the major flood event that occurred in June 2016, during which water levels reached almost 1 m above the ground in s4 (data not shown here).

5 | CONCLUSION

The effect of water table dynamics on chloride concentrations in a riparian peatland was studied during a three-year monitoring period. Strong water table fluctuations characterize the site, alternating between low and high water tables, driven by the seasonal vegetation life cycle. The use of stable water isotopes was essential for understanding the system's hydrogeological functioning, in which the river is crucial in compensating for the transpiration of plants during the dry season. This study also illustrates that chloride is not genuinely conservative in such environments if only the saturated zone is considered. The unsaturated zone and water table dynamics are crucial in controlling the chloride concentrations of shallow groundwater in peatlands. As illustrated in Figure 8, the variations in chloride concentration show vertical processes. It implies chloride accumulation within the unsaturated zone during the summer when the water table is low and transfers to the saturated zone when the water table rises. They also show lateral processes with chloride transfer induced by asynchronous rewetting dynamics from zones where the water table recovers faster to zones where it recovers more slowly. In such heterogeneous environments, having enough spatially distributed sampling points to understand processes associated with water table dynamics is therefore essential. In this context, multiplying unsaturated zone water sampling points at different observation locations could help constrain the various assumptions developed in this work and provide a fuller picture of chloride behaviour in a riparian peatland subject to high water table fluctuations.

ACKNOWLEDGEMENTS

The authors thank the Essonne River syndicate (SIARCE), particularly M. Sahaghian, for permitting these experiments in the Jarcy peatland and supporting their implementation. This work received support from the Université Paris-Saclay, through the program Emergence 2018 and 2019 (ONARIE). They are also grateful to the many students and colleagues who helped us in the field during the three-year monitoring period. Finally, the authors thank the Academic Writing Center of the University Paris-Saclay, which assisted them in the proofreading of this manuscript.

DATA AVAILABILITY STATEMENT

The data that support the findings of this study are available from the corresponding author upon reasonable request.

ORCID

Adrien Renaud  <https://orcid.org/0000-0003-3733-4701>

Véronique Durand  <https://orcid.org/0000-0002-5816-9306>

Claude Mügler  <https://orcid.org/0000-0003-3129-7348>

Emmanuel Léger  <https://orcid.org/0000-0001-7669-3622>

ENDNOTE

¹ The data used in this work were collected on the Fontainebleau (IAEA/WMO, 2022) site which belongs to the National Observation Service (SNO) RENOIR (French network of isotopes in precipitation; <https://sno-renoir.osups.universite-paris-saclay.fr>) funded by the Institute of Sciences of the Universe of the National Center for Scientific Research (INSU/CNRS), and which aims to strengthen the sharing of knowledge and to promote multidisciplinary research on the “Entry” function of hydro-eco-cryo-systems.

REFERENCES

- Ahmad, S., Liu, H., Alam, S., Günther, A., Jurasinski, G., & Lennartz, B. (2021). Meteorological controls on water table dynamics in fen peatlands depend on management regimes. *Frontiers in Earth Science*, 9, 630469.
- Aubert, A. H., Gascuel-Oudou, C., Gruau, G., Akkal, N., Fauchoux, M., Fauvel, Y., Grimaldi, C., Hamon, Y., Jaffrézic, A., Lecoz-Boutnik, M., Molenat, J., Petitjean, P., Ruiz, L., & Merot, P. (2013). Solute transport dynamics in small, shallow groundwater-dominated agricultural catchments: Insights from a high-frequency, multi-solute 10 yr-long monitoring study. *Hydrology and Earth System Sciences*, 17(4), 1379–1391.
- Auterives, C., Aquilina, L., Bour, O., Davranche, M., & Paquereau, V. (2011). Contribution of climatic and anthropogenic effects to the hydric deficit of peatlands. *Hydrological Processes*, 25, 2890–2906.
- Balliston, N., & Price, J. (2020). Heterogeneity of the peat profile and its role in unsaturated sodium chloride rise at field and laboratory scales. *Vadose Zone Journal*, 19, e20015.
- Belyea, L. R., & Malmer, N. (2004). Carbon sequestration in peatland: Patterns and mechanisms of response to climate change. *Global Change Biology*, 10(7), 1043–1052.
- Beysens, D., Mongruel, A., & Acker, K. (2017). Urban dew and rain in Paris, France: Occurrence and physico-chemical characteristics. *Atmospheric Research*, 189, 152–161.
- Biester, H., Selimović, D., Hemmerich, S., & Petri, M. (2006). Halogens in pore water of peat bogs – The role of peat decomposition and dissolved organic matter. *Biogeosciences*, 3(1), 53–64.
- Blodau, C., Mayer, B., Peiffer, S., & Moore, T. R. (2007). Support for an anaerobic sulfur cycle in two Canadian peatland soils. *Journal of Geophysical Research: Biogeosciences*, 112(G2).
- Burt, T. P., Pinay, G., Matheson, F. E., Haycock, N. E., Butturini, A., Clement, J. C., Danielescu, S., Dowrick, D. J., Hefting, M. M., Hillbricht-Ilkowska, A., & Maitre, V. (2002). Water table fluctuations in the riparian zone: Comparative results from a pan-european experiment. *Journal of Hydrology*, 265, 129–148.
- Carlson Mazur, M. L., Wiley, M. J., & Wilcox, D. A. (2014). Estimating evapotranspiration and groundwater flow from water-table fluctuations for a general wetland scenario. *Ecohydrology*, 7(2), 378–390.
- Charman, D. J., Joosten, H., Laine, J., Lee, D., Minayeva, T., Opdam, S., Parish, F., Silvius, M., & Sirin, A. (2008). *Assessment on peatlands, biodiversity and climate change*. Technical report. Global Environment Centre & Wetlands International.
- Cirkel, D., Beek, C., Witte, J.-P., & van der Zee, S. (2014). Sulphate reduction and calcite precipitation in relation to internal eutrophication of groundwater fed alkaline fens. *Biogeochemistry*, 117, 375–393.
- Clay, A., Bradley, C., Gerrard, A. J., & Leng, M. J. (2004). Using stable isotopes of water to infer wetland hydrological dynamics. *Hydrology and Earth System Sciences Discussions*, 8(6), 1164–1173. Publisher: European Geosciences Union.
- Clement, J.-C., Pinay, G., & Marmonier, P. (2002). Seasonal dynamics of denitrification along topo-hydrosequences in three different riparian wetlands. *Journal of Environmental Quality*, 31(3), 1025–1037.
- Convention on Wetlands. (2021). *Global wetland outlook: Special edition 2021*. Technical report.
- Craig, H. (1961). Isotopic variations in meteoric waters. *Science*, 133(3465), 1702–1703. Publisher: American Association for the Advancement of Science, 133, 1702, 1703.
- De Ridder, J. (2012). *Reponse des processus biochimiques d'une tourbière soumise à des fluctuations du niveau d'eau*. Theses (p. 1). Université Rennes.
- Engloner, A. I. (2009). Structure, growth dynamics and biomass of reed (*Phragmites australis*) – A review. *Flora - Morphology, Distribution, Functional Ecology of Plants*, 204(5), 331–346.
- Freeman, C., Lock, M. A., & Reynolds, B. (1993). Climatic change and the release of immobilized nutrients from Welsh riparian wetland soils. *Ecological Engineering*, 2(4), 367–373.
- Gaberščik, A., Grašič, M., Abram, D., & Zelnik, I. (2020). Water level fluctuations and air temperatures affect common reed habitus and productivity in an intermittent wetland ecosystem. *Water*, 12, 2806.
- Gourcy, L., & Brenot, A. (2011). Multiple environmental tracers for a better understanding of water flux in a wetland area (La Bassée, France). *Applied Geochemistry*, 26(12), 2147–2158.
- Griffiths, N. A., Sebestyen, S. D., & Oleheiser, K. C. (2019). Variation in peatland porewater chemistry over time and space along a bog to fen gradient. *Science of the Total Environment*, 697, 134152.
- Grimaldi, C., Thomas, Z., Fossey, M., Fauvel, Y., & Merot, P. (2009). High chloride concentrations in the soil and groundwater under an oak hedge in the west of France: An indicator of evapotranspiration and water movement. *Hydrological Processes*, 23, 1865–1873.
- Gustavsson, M., Karlsson, S., Oeberg, G., Sanden, P., Svensson, T., Valinia, S., Thiry, Y., & Bastviken, D. (2012). Organic matter chlorination rates in different boreal soils: The role of soil organic matter content. *Environmental Science and Technology*, 46(3), 1504–1510. Funding Agencies Swedish Research Council (VR) 2006–5387.
- Hao, H., Grimaldi, C., Walter, C., Dutin, G., Trinkl, B., & Merot, P. (2015). Chloride concentration distribution under oak hedgerow: An indicator of the water-uptake zone of tree roots? *Plant and Soil*, 386(1), 357–369.
- Hayashi, M., Kamp, G. v. d., & Rudolph, D. L. (1998). Water and solute transfer between a prairie wetland and adjacent uplands, 1. Water balance. *Journal of Hydrology*, 207(1), 42–55.
- Heitman, J., Horton, R., Sauer, T., & DeSutter, T. (2008). Sensible heat observations reveal soil-water evaporation dynamics. *Journal of Hydro-meteorology*, 9, 165–171.
- Holden, J., Chapman, P., & Labadz, J. (2003). Artificial drainage of peatlands: Hydrological and hydrochemical process and wetland restoration. *Progress in Physical Geography*, 28, 95–123.
- Humphries, M. S., Kindness, A., Ellery, W., Hughes, J., Bond, J., & Barnes, K. (2011). Vegetation influences on groundwater salinity and chemical heterogeneity in a freshwater, recharge floodplain wetland, South Africa. *Journal of Hydrology*, 411, 130–139.
- IAEA/WMO. (2022). *Global network of isotopes in precipitation. the gnip database*.
- IPCC. (2022). *Summary for policymakers* (pp. 1–24). Cambridge University Press.
- Isokangas, E., Rossi, P., Ronkanen, A.-K., Marttila, H., Rozanski, K., & Klöve, B. (2017). Quantifying spatial groundwater dependence in

- peatlands through a distributed isotope mass balance approach. *Water Resources Research*, 53, 2524–2541.
- Joris, I., & Feyen, J. (2003). Modeling water flow and seasonal soil moisture dynamics in an alluvial groundwater-fed wetland. *Hydrology and Earth System Sciences*, 7, 57–66.
- Kashparov, V., Colle, C., Levchuk, S., Yoschenko, V., & Zvarich, S. (2007). Radiochlorine concentration ratios for agricultural plants in various soil conditions. *Journal of Environmental Radioactivity*, 95(1), 10–22.
- Kirchner, J., & Tetzlaff, D. (2010). Chloride and water isotopes as tracers of storage and mixing in two scottish catchments. *Hydrological Processes*, 24, 1631–1645.
- Liebhart, G., Klik, A., Stumpp, C., & Nolz, R. (2022). Partitioning evapotranspiration using water stable isotopes and information from lysimeter experiments. *Hydrological Sciences Journal*, 67, 1–16.
- Lovett, G. M., Likens, G. E., Buso, D. C., Driscoll, C. T., & Bailey, S. W. (2005). The biogeochemistry of chlorine at Hubbard brook, New Hampshire, USA. *Biogeochemistry*, 72(2), 191–232.
- McCarter, C. P. R., Rezanezhad, F., Gharedaghloo, B., Price, J. S., & Cappellen, P. V. (2019). Transport of chloride and deuterated water in peat: The role of anion exclusion, diffusion, and anion adsorption in a dual porosity organic media. *Journal of Contaminant Hydrology*, 225, 103497.
- McLaughlin, J., & Webster, K. (2010). Alkalinity and acidity cycling and fluxes in an intermediate fen peatland in northern Ontario. *Biogeochemistry*, 99, 143–155.
- Montelius, M., Svensson, T., LouriBo-Cabana, B., Thiry, Y., & Bastviken, D. (2019). Radiotracer evidence that the rhizosphere is a hot-spot for chlorination of soil organic matter. *Plant and Soil*, 443, 245–257.
- Myneni, S. C. B. (2002). Formation of stable chlorinated hydrocarbons in weathering plant material. *Science*, 295(5557), 1039–1041. Publisher: American Association for the Advancement of Science, 295, 1039, 1041.
- Ng, G.-H. C., Yourd, A. R., Johnson, N. W., & Myrbo, A. E. (2017). Modeling hydrologic controls on sulfur processes in sulfate-impacted wetland and stream sediments. *Journal of Geophysical Research: Biogeosciences*, 122(9), 2435–2457.
- Öberg, G., & Grøn, C. (1998). Sources of organic halogens in spruce Forest soil. *Environmental Science & Technology*, 32(11), 573–1579. Publisher: American Chemical Society, 32, 1573, 1579.
- Quenet, M., Celle-Jeanton, H., Voltaire, O., Albaric, J., Huneau, F., Peiry, J.-L., Allain, E., Garreau, A., & Beauger, A. (2019). Coupling hydrodynamic, geochemical and isotopic approaches to evaluate oxbow connection degree to the main stream and to adjunct alluvial aquifer. *Journal of Hydrology*, 577, 123936.
- Reddy, M. M., Reddy, M. B., Kipp, K. L., Burman, A., Schuster, P., & Rawlik, P. S., Jr. (2008). Peat predate chloride concentration profiles in the Everglades during wet/dry cycles from January 1996 to June 1998: Field measurements and theoretical analysis. *Hydrological Processes*, 22(11), 1713–1724. <https://doi.org/10.1002/hyp.6739>
- Redon, P.-O., Jolivet, C., Saby, N. P. A., Abdelouas, A., & Thiry, Y. (2013). Occurrence of natural organic chlorine in soils for different land uses. *Biogeochemistry*, 114(1), 413–419.
- Renee Brooks, J., Barnard, H. R., Coulombe, R., & McDonnell, J. J. (2010). Ecohydrologic separation of water between trees and streams in a Mediterranean climate. *Nature Geoscience*, 3(2), 100–104.
- Rubol, S., Silver, W., & Bellin, A. (2012). Hydrologic control on redox and nitrogen dynamics in a peatland soil. *The Science of the Total Environment*, 432, 37–46.
- Schilling, K. (2007). Water table fluctuations under three riparian land covers, Iowa (USA). *Hydrological Processes*, 21, 2415–2424.
- Svensson, T., Kylin, H., Montelius, M., Sandén, P., & Bastviken, D. (2021). Chlorine cycling and the fate of Cl in terrestrial environments. Technical report.
- Urban, N. R., Eisenreich, S. J., & Grigal, D. F. (1989). Sulfur cycling in a forested sphagnum bog in northern Minnesota. *Biogeochemistry*, 7(2), 81–109.
- Vargas, A. I., Schaffer, B., Yuhong, L., & da Silveira Lobo Sternberg, L. (2017). Testing plant use of mobile vs immobile soil water sources using stable isotope experiments. *New Phytologist*, 215(2), 582–594.
- Verhagen, F. J. M., Swarts, H. J., Wunberg, J. B. P. A., & Field, J. A. (1998). Organohalogen production is a ubiquitous capacity among basidiomycetes. *Chemosphere*, 37(9), 2091–2104.
- Volik, O., Kessel, E., Green, A., Petrone, R., & Price, J. (2020). Growingseason evapotranspiration in boreal fens in the athabasca oil sands region: Variability and environmental controls. *Hydrological Processes*, 35, e14020.
- Vreca, P., & Kern, Z. (2020). Use of water isotopes in hydrological processes. *Water*, 12(8), 1–6.
- Warren, F. J., Waddington, J. M., Bourbonniere, R. A., & Day, S. M. (2001). Effect of drought on hydrology and sulphate dynamics in a temperate swamp. *Hydrological Processes*, 15(16), 3133–3150.
- Zhao, X., Xia, J., Chen, W., Chen, Y., Fang, Y., & Qu, F. (2019). Transport characteristics of salt ions in soil columns planted with tamarix chinensis under different groundwater levels. *PLoS One*, 14(4), 1–17.
- Zimmermann, U., Ehhalt, D., and Muennich, K. O. (1968). *Soil-water movement and evapotranspiration: Changes in the isotopic composition of the water*. International Atomic Energy Agency (AIEA).

How to cite this article: Renaud, A., Durand, V., Mügler, C., Marlin, C., Léger, E., Noret, A., & Monvoisin, G. (2023). Influence of vegetation-induced water table seasonality on groundwater chloride concentration dynamics in a riparian fen peatland. *Hydrological Processes*, 37(12), e15054. <https://doi.org/10.1002/hyp.15054>

APPENDIX A

